Preparation, Crystal Structure and Single-crystal Polarized Spectra of Bis(1,2,6,7-tetracyano-3,5-dihydro-3,5-diimino-pyrrolizinido)zinc(II)–Tetrahydrofuran (1/4)†

Vincenzo Fares,*[a] Alberto Flamini,*[a] Jill R. Jasin,[b] Ronald L. Musselman*[b] and Nicola Poli[a]

[a] *Institute of Materials Chemistry, CNR, Research Area of Rome, PO Box 10, 00016 Monterotondo Stazione, Rome, Italy*

[b] *Department of Chemistry, Franklin and Marshall College, Lancaster, Pennsylvania 17604, USA*

The complex bis(1,2,6,7-tetracyano-3,5-dihydro-3,5-diiminopyrrolizinido)zinc(II), as its tetrahydrofuran (thf) adduct, $Zn(C_{11}N_7H_2)_2 \cdot 4thf$, has been synthesized and its crystal structure determined. The zinc atom, which lies on a crystallographic symmetry centre, co-ordinates four imino groups in a square-planar arrangement [Zn–N_{imino} 2.070(8) Å] and two thf units in the apical positions [Zn–O_{thf} 2.249(7) Å]; the other two thf molecules are equatorially linked to the imino hydrogens. The electronic absorption spectra have been derived through a Kramers–Krönig transformation of the single crystal polarized specular reflectance spectra and then resolved *via* Gaussian deconvolution. They show an extensive mixed polarization, since their prominent components are distributed along different molecular directions. The low-energy band (Q) is polarized mainly along the in-plane molecular short axis (y), the next band (B) along the long axis (x) and the third band (N) along z. The interpretation is based on the only available theoretical model, that is INDO/S molecular orbital calculations, carried out on the analogous Ni^{II} complex (D_{2h}). The agreement between the observed and predicted transitions is qualitatively quite good, in the sense that several spectroscopic states have been calculated within the energy range investigated, of symmetry mainly $B_{2u}(y)$ at low energy, $B_{3u}(x)$ at intermediate energy and $B_{1u}(z)$ at high energy. While crystal optics may contribute slightly to polarization mixing, there is evidence for vibronic coupling between states of different symmetry; the proposed assignment (D_{2h}) is thus based on the extrapolation of the above calculations by using the vibronic coupling, with the frequent occurrence of the type $B_{2u} \times b_{1g} \times B_{3u}$.

The complexes $[ML_2]$ (L = 1,2,6,7-tetracyano-3,5-dihydro-3,5-diiminopyrrolizinide), which some of us synthesized for the first time recently,[1] are interesting as they show optical spectra extraordinarily similar to those of the corresponding phthalocyaninates [M(pc)].[2] Molecular orbital calculations by Nakamura *et al.*[3] on the two systems $[ML_2]$ and [M(pc)] (M = Ni) successfully explained such similarity; an important result of the calculations was that the Q band in $[ML_2]$ (D_{2h}) should be polarized along the shorter molecular axis (y). Such a property, which [M(pc)] complexes do not have because of their higher symmetry (D_{4h}), is very important and eventually could be exploited profitably in some electrooptical applications, where, for instance, $[ML_2]$ species are used as guest molecules in oriented matrices.[4] In order to test the calculations and to establish the polarization properties of the Q band in $[ML_2]$ complexes on an experimental basis, we have for some time been studying this type of system. We have therefore synthesized and characterized the $[ZnL_2]$ complex, which shows an optical spectrum very similar to that of [Zn(pc)], particularly in the low-energy region up to *ca.* 25 × 10^3 cm^{-1} (Fig. 1). Moreover its tetrahydrofuran (thf) adduct is suitable for polarization measurements, as there is only one molecule in the unit cell.

In this paper we report the synthesis, crystal structure and polarized single-crystal reflection spectra of the adduct $ZnL_2 \cdot 4thf$. We also discuss the spectroscopic results in relation to the theoretical calculations of Nakamura *et al.*,[3] and draw conclusions about both the observed polarization and probable assignment.

† *Supplementary data available:* see Instructions for Authors, *J. Chem. Soc., Dalton Trans.*, 1995, Issue 1, pp. xxv–xxx.

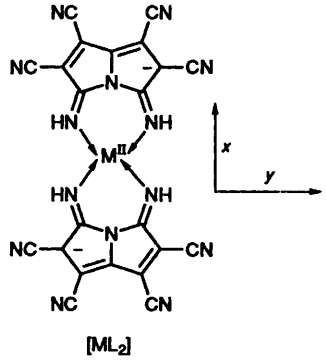

$[ML_2]$

Experimental

Materials.—Solvents were carefully dried, freshly distilled and degassed before use. The compound NaL was prepared according to our procedure.[5] Anhydrous $ZnCl_2$ was prepared from commercial $ZnCl_2 \cdot xH_2O$ with $SOCl_2$.[6]

Synthesis of $ZnL_2 \cdot 4thf$.—An amount of NaL (0.5 g, 1.96 mmol) was dissolved in anhydrous thf (30 cm^3) and anhydrous $ZnCl_2$ (0.5 g, 3.67 mmol) added under N_2 at room temperature. The resulting intense blue solution was stirred for 30 min. On addition of anhydrous CH_2Cl_2 (50 cm^3) a bronze microcrystalline precipitate formed, which was filtered off and washed with water. After refluxing with thf for 10 min and filtering, $ZnL_2 \cdot 4thf$ was obtained as bronze microcrystals (0.68 g, 85%). Suitable crystals for both spectroscopic and X-ray diffraction

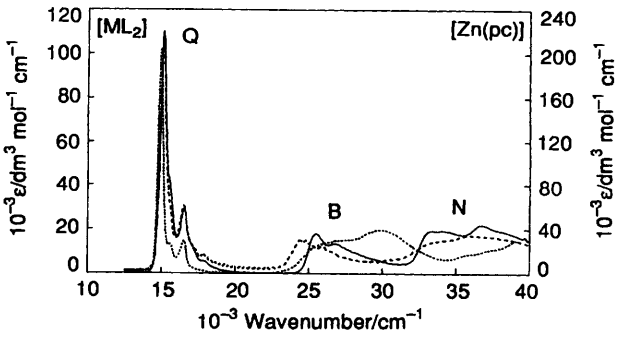

Fig. 1 Solution electronic spectra of [Zn(pc)] (····) in dimethylacetamide, [NiL_2] (– – – –) 1.24 × 10^{-4} mol dm^{-3} in methanol–water (5:1) + 0.2 mol dm^{-3} $NiCl_2·6H_2O$, and [ZnL_2] (———) 1.77 × 10^{-4} mol dm^{-3} in thf + 0.2 mol dm^{-3} $ZnCl_2$

studies were grown in a sealed vial from a saturated hot solution of thf–toluene (5:2), by slow cooling from 80 °C to room temperature over 7 d. The elemental analyses were not reproducible owing to the partial loss of thf when the sample was dried; however, the experimental X-ray powder diffraction patterns from freshly prepared samples were reproducible and in agreement with the diffraction patterns calculated from single-crystal analysis.[7]

X-Ray Crystallography.—Data collection. A plate-like, single crystal of $ZnL_2·4thf$, of dimensions 0.5 × 0.3 × 0.05 mm, was embedded in silicone grease inside a glass capillary in the presence of mother-liquor. Preliminary oscillation and Weissenberg photographs indicated a triclinic symmetry and the well developed crystal face coincident with the (001) plane, the long and short edges being parallel to the *y* and *x* crystallographic directions (Fig. 4, insert).

Data were collected using a Nicolet $P2_1$ four-circle automated diffractometer in the θ–2θ scan mode and with graphite-monochromated Mo-Kα radiation; 4032 reflections with $3.0 < 2\theta < 50.0°$ were examined. Two standard reflections were measured every 50 during data collection and showed no significant variation in intensity. Data were corrected for Lorentz and polarization factors; a semiempirical absorption correction was also applied, based on azimuthal scan data from selected reflections. Unit-cell parameters were derived from 25 accurately centred medium-angle reflections ($16 < 2\theta < 26°$). The crystal data and details of data collection are given in Table 1.

Solution and refinement of the structure. The structure was solved by conventional Patterson and Fourier methods and refined by full-matrix least-square methods. The final refinements were made with anisotropic thermal parameters for non-hydrogen atoms; hydrogens, placed in their geometrical calculated positions, were restrained to ride on their associated carbon or nitrogen atoms. The quantity minimized was $\Sigma w(|F_o| - |F_c|)^2$ where $w^{-1} = \sigma^2(F_o) + 0.004\,F_o^2$. Residuals R ($= \Sigma||F_o| - |F_c||/\Sigma|F_o|$) and R' $\{= [\Sigma w(|F_o| - |F_c|)^2/\Sigma w|F_o|^2]^{\frac{1}{2}}\}$ were 0.064 and 0.050, respectively. Neutral scattering factors, f' and f'' values, were those from the literature.[8] All calculations were carried out using the PC version of the SIR-CAOS Crystallographic Program System.[9] Final atomic positional parameters for the non-hydrogen atoms are given in Table 2.

Additional material available from the Cambridge Crystallographic Data Centre comprises H-atom coordinates and thermal parameters.

Single-crystal Spectral Measurements.—Due to the high absorption coefficients for this system, polarized spectra were obtained through specular reflectance rather than transmission. The reflectance instrument, based on a concept by Anex,[10] is essentially a grating microspectrophotometer consisting of tungsten-halogen and xenon arc light sources, an Instruments SA HR320 0.32 m computer-controllable grating monochromator, a Glan–Thompson polarizer, a double-beam reflecting microscope and a photomultiplier detector. Signal detection is through two Princeton Applied Research 186A lock-in amplifiers, and instrument control resides on an Apple IIe computer. Data for each spectral point are collected until the sample mean has a 99% probability of being within 1% of the population mean. The data are then uploaded to a Hewlett-Packard 3000 computer for processing. Reflectance is measured relative to an NIST standard second-surface mirror, and Kramers–Krönig transformation of the average of at least three reflectance spectra is performed to obtain standard absorbance values. An effective transition was added in the region at higher energies than measured in order to allow proper transformation of the ultraviolet region, determined to be suitable when the valleys in the transformed data resembled those from solution

Table 1 Crystal data for $ZnL_2·4thf$

Formula	$C_{38}H_{36}N_{14}O_4Zn$
M	818.2
a/Å	9.949(2)
b/Å	10.972(3)
c/Å	11.544(4)
α/°	97.47(2)
β/°	109.96(2)
γ/°	113.63(2)
U/Å^3	1031.7(5)
Z	1
D_c/g cm^{-3}	1.317
Space group	$P\bar{1}$
Radiation (λ, Å)	Mo-Kα (0.710 69)
μ/cm^{-1}	6.62
F(000)	424
Transmission coefficients	0.85–0.98
R	0.0644
R'	0.0501

Table 2 Atomic coordinates for $ZnL_2·4thf$ with estimated standard deviation (e.s.d.s) in parentheses

Atom	x	y	z
Zn	0.0000	0.0000	0.0000
N(1)	−0.1707(7)	−0.1724(7)	0.1660(6)
C(2)	−0.1792(9)	−0.2591(9)	0.0596(7)
C(3)	−0.2645(8)	−0.3981(9)	0.0718(8)
C(4)	−0.3015(9)	−0.389(1)	0.1796(8)
C(5)	−0.2422(9)	−0.245(1)	0.2368(8)
C(6)	−0.2256(9)	−0.147(1)	0.3372(8)
C(7)	−0.1403(9)	−0.013(1)	0.3285(7)
N(8)	−0.1242(7)	−0.2098(6)	−0.0184(6)
C(9)	−0.3050(9)	−0.5265(9)	−0.0147(8)
C(10)	−0.383(1)	−0.500(1)	0.2229(9)
C(11)	−0.287(1)	−0.178(1)	0.433(1)
C(12)	−0.0955(9)	0.116(1)	0.4109(7)
C(13)	−0.1011(8)	−0.0276(8)	0.2181(8)
N(14)	−0.0269(7)	0.0561(6)	0.1658(6)
N(15)	−0.3353(9)	−0.6264(7)	−0.0844(7)
N(16)	−0.446(1)	−0.5888(9)	0.2545(9)
N(17)	−0.331(1)	−0.198(1)	0.5095(8)
N(18)	−0.0599(8)	0.2222(8)	0.4778(7)
O(101)	0.2318(6)	−0.0026(5)	0.1153(5)
C(102)	0.266(1)	−0.048(2)	0.218(1)
C(103)	0.442(2)	0.001(2)	0.288(1)
C(104)	0.497(1)	0.031(2)	0.198(1)
C(105)	0.368(1)	0.039(1)	0.093(1)
O(201)	0.1163(7)	0.3663(5)	0.2457(5)
C(202)	0.255(1)	0.463(1)	0.3625(8)
C(203)	0.224(1)	0.575(1)	0.399(1)
C(204)	0.072(2)	0.547(1)	0.303(1)
C(205)	0.001(1)	0.415(1)	0.2131(9)

data. The effective transitions had no effect on energies of transitions, but did affect baselines.

Polarized single-crystal specular reflectance spectra were taken for the two natural faces (001) and (100) with the electric vectors parallel to, and at 90° from the [010] direction, respectively. The molecular coordinate system used was defined with y along the shorter in-plane molecular axis.

Results and Discussion

Description of the Structure.—The structure of ZnL_2·4thf consists of isolated centrosymmetric complex units. The metal atom is six-co-ordinated in a tetragonally elongated octahedral geometry (Fig. 2), being surrounded by four imino nitrogen atoms in a square-planar arrangement at a mean distance of 2.070(8) Å and by two thf oxygen atoms in the apical positions, at a distance of 2.249(7) Å; the other two thf molecules are equatorially linked to the imino hydrogens *via* the oxygen atoms (H_{imino}–O_{thf} 1.94 Å). The Zn–O apical distance is comparable with those found in other octahedral zinc complexes with the same N_4O_2 atom donor set[11,12] (range 2.15–2.41 Å), while the Zn–N_{imino} distance is shorter than that present both in the above mentioned ZnN_4O_2 complexes (range 2.089–2.227 Å), and in other zinc six-co-ordinate aza complexes,[13] where the values observed fall in the range 2.095–2.479 Å, but where however, the nitrogen atom is sp^3 hybridized. Other (four- or five-co-ordinate) Zn–N_{sp^2} complexes show a wider range of Zn–N values between 1.98 and 2.17 Å.[14] The main interatomic distances and angles are reported in Table 3. The Zn atom lies on a crystallographic centre of symmetry, so that the ZnN_4 equatorial group does not show any out-of-plane distortion. On the whole, the ZnL_2 complex unit strictly resembles the analogous NiL_2 unit found in the octahedral complex NiL_2·$2H_2O$·$3C_4H_8O_2$,[2] thus confirming the correlation between the electronic distribution within the complex (intramolecular distances) and the metal co-ordination geometry. The presence of two independent five-atom thf rings, which have an intrinsically disordered twist/envelope conformation,[15] slightly affects the results so that large standard deviations and high thermal parameters are found (Tables 2, 3 and Fig. 3).

Electronic Spectra.—The reflection spectra for the (100) face, which exhibits a better dichroism than the other face (001) examined, are reported in Fig. 4. The principal directions were empirically determined by measuring the positions of maximum (R_{max}) and minimum (R_{min}) reflectivity at 14.4 × 10^3 cm^{-1}; for the two curves the incident radiation was polarized parallel to the R_{max} ($R2$) and to R_{min} ($R1$) direction, respectively. It is to be noted that, while the triclinic nature of this crystal allows for the possibility of rotation of the electric vectors upon transmission through the crystal, the strong absorbances involved here minimize such polarization rotation since the specular

Table 3 Bond lengths (Å) and angles (°) for ZnL_2·4thf with e.s.d.s in parentheses

Zn–N(8)	2.070(8)	C(7)–C(13)	1.46(1)
Zn–N(14)	2.071(6)	C(9)–N(15)	1.13(2)
Zn–O(101)	2.249(7)	C(10)–N(16)	1.11(2)
N(1)–C(2)	1.41(1)	C(11)–N(17)	1.12(1)
N(1)–C(5)	1.39(1)	C(12)–N(18)	1.15(2)
N(1)–C(13)	1.40(2)	C(13)–N(14)	1.29(1)
C(2)–C(3)	1.47(2)	O(101)–C(102)	1.34(2)
C(2)–N(8)	1.28(1)	O(101)–C(105)	1.37(2)
C(3)–C(4)	1.42(1)	C(102)–C(103)	1.47(3)
C(3)–C(9)	1.43(2)	C(103)–C(104)	1.34(2)
C(4)–C(5)	1.41(2)	C(104)–C(105)	1.48(2)
C(4)–C(10)	1.43(2)	O(201)–C(202)	1.43(2)
C(5)–C(6)	1.40(2)	O(201)–C(205)	1.42(1)
C(6)–C(7)	1.41(2)	C(202)–C(203)	1.43(1)
C(6)–C(11)	1.45(1)	C(203)–C(204)	1.42(3)
C(7)–C(12)	1.40(2)	C(204)–C(205)	1.40(2)
N(14)–Zn–N(8)	90.8(3)	N(15)–C(9)–C(3)	179(1)
O(101)–Zn–N(8)	87.9(3)	N(16)–C(10)–C(4)	178(1)
O(101)–Zn–N(14)	91.8(3)	N(17)–C(11)–C(6)	178(1)
C(5)–N(1)–C(2)	114(1)	N(18)–C(12)–C(7)	179(1)
C(13)–N(1)–C(2)	133.5(8)	C(7)–C(13)–N(1)	103.0(8)
C(13)–N(1)–C(5)	112.9(8)	N(14)–C(13)–N(1)	121.0(8)
C(3)–C(2)–N(1)	101.0(7)	C(105)–O(101)–C(102)	105(1)
N(8)–C(2)–N(1)	122(1)	C(103)–C(102)–O(101)	111(1)
N(8)–C(2)–C(3)	137(1)	C(104)–C(103)–C(102)	103(1)
C(4)–C(3)–C(2)	112(1)	C(105)–C(104)–C(103)	107(1)
C(5)–C(4)–C(3)	106(1)	C(104)–C(105)–O(101)	109(1)
C(4)–C(5)–N(1)	108.1(8)	C(205)–O(201)–C(202)	109.3(9)
C(6)–C(5)–N(1)	107(1)	C(203)–C(202)–O(201)	106(1)
C(7)–C(6)–C(5)	108.2(8)	C(204)–C(203)–C(202)	108(1)
C(13)–C(7)–C(6)	109(1)	C(205)–C(204)–C(203)	109(1)
		C(204)–C(205)–O(201)	107(1)

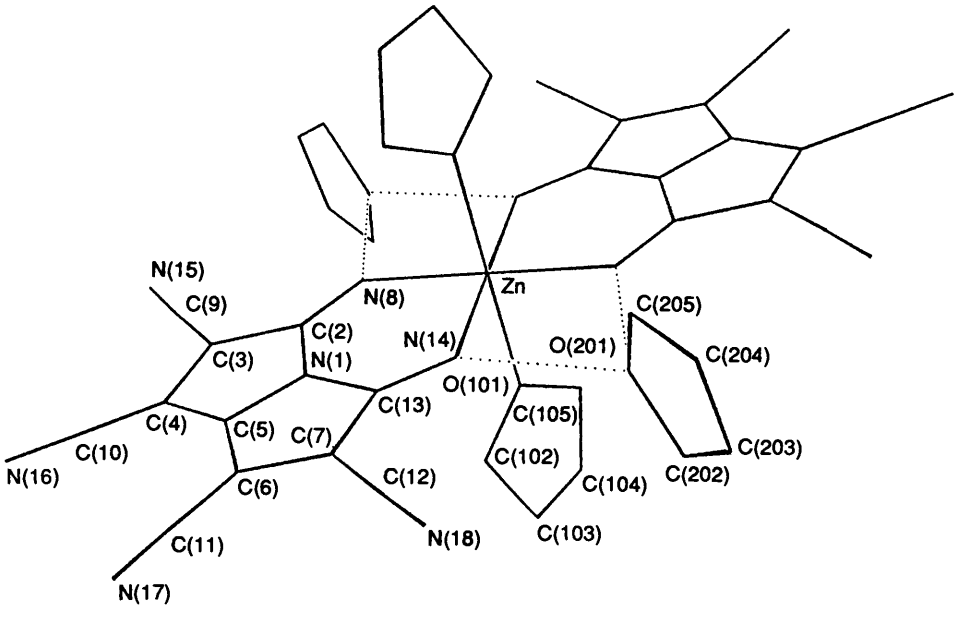

Fig. 2 Schematic view and labelling scheme of ZnL_2·4thf

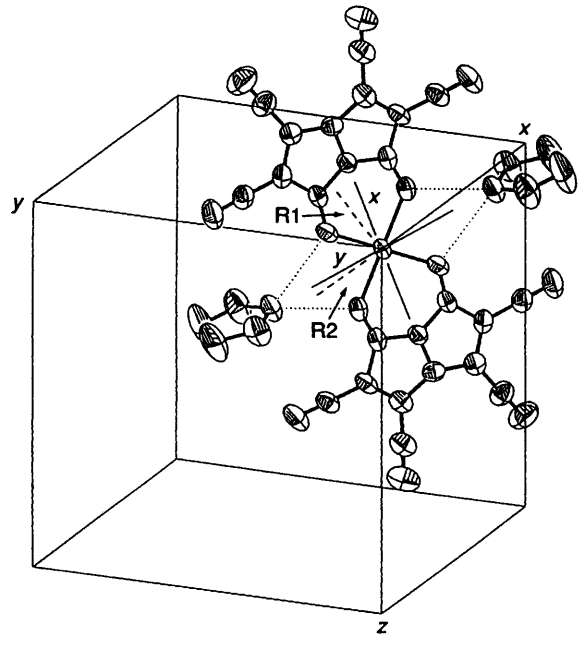

Fig. 3 Projection of the unit cell of ZnL_2·4thf (apical thf molecules excluded) onto the (100) plane in which the *R*1 and *R*2 polarization directions are shown together with the *x* and *y* molecular axes

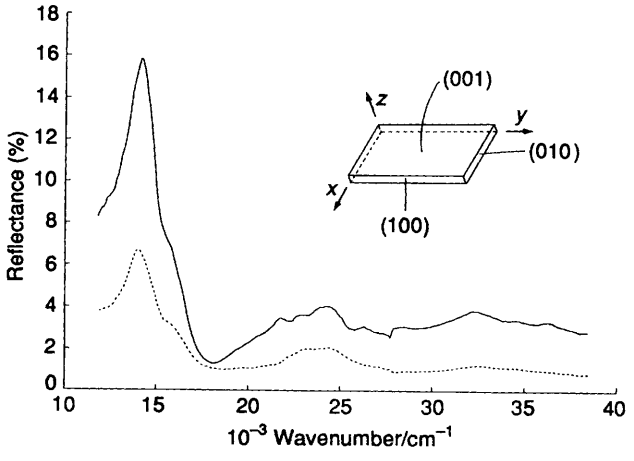

Fig. 4 Single-crystal polarized specular reflectance on the narrow (100) face of ZnL_2·4thf; (———) electric vector parallel to the *R*2 direction; (– – –) electric vector parallel to *R*1. The insert shows the plate-like crystal morphology and its relationship with crystallographic planes and directions

reflectance process occurs close to the crystal surface. Polarization *R*1 was essentially along the molecular *x* axis, and polarization *R*2 along *y*. Specifically, the contributions to the intensities were: $IR1 = 0.759\ I_x + 0.016\ I_y + 0.223\ I_z$ and $IR2 = 0.058\ I_x + 0.909\ I_y + 0.034\ I_z$. The situation is shown in Fig. 3. The major features of the absorption curves are summarized graphically in Figs. 5 and 6 and numerically in Table 4. It should be noted that the residual baselines at low energies in Figs. 5 and 6 may have resulted from having assumed a flat reflectance throughout the IR region for the Kramers–Krönig transformations.

The reported spectra consist of three main bands, labelled Q, B and N, by analogy with [M(pc)]. After inspection of the variation of the relative areas on changing *R* (Table 4) and comparison with the spectra taken on the (001) face (see below), it is clear that the bands are only partially polarized (along *y*, *x* and *z*, respectively), because of the occurrence of extensive mixed polarization. The dominant *z* polarization of the N band

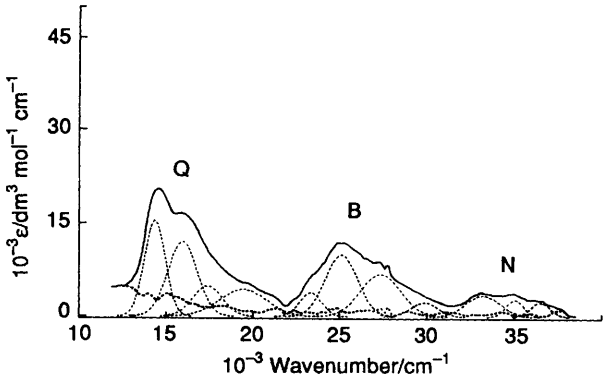

Fig. 5 Kramers–Krönig transformed spectrum of ZnL_2·4thf, with the electric vector parallel to *R*1 and Gaussian analyses: (———) transformed experimental spectrum; (- - - -) Gaussian curve; (• • • •) residual

emerges from a comparison of the present spectra, which are essentially in-plane spectra ($I_z \leqslant 0.23$), with the spectrum (not shown) taken on the (001) face with the electric vector at 90° from the *b* axis, which contain a much higher fraction of *z* polarized light ($I_z = 0.47$). Interestingly, in the latter spectrum the total area of the N band increases considerably in comparison with those of Q and B. Moreover, it is particularly interesting that some spectral differences emerge when the crystal and solution spectra are compared: (*i*) the intensity of the N band is sharply reduced in the crystal, probably because this band originates also by *z* polarized transitions as already discussed, and (*ii*) the Q band is broader and shifted to the red by about 700 cm^{-1} in the crystal, presumably because of the exchange of phonons with the lattice.

Theoretical Model.—The only theoretical mode available for interpretation of the observed spectra is that of Nakamura *et al.*,[3] namely molecular orbital calculations performed with the INDO/S (ZINDO) method on $[NiL_2]$ (D_{2h}). Such a model also appears to be a plausible starting point for the interpretation of the electronic properties of ZnL_2·4thf, treated as if it were $[ZnL_2]$ (D_{2h}), since (*i*) the two $[ML_2]$ (M = Ni or Zn) compounds have almost identical solution spectra (Fig. 1), (*ii*) the spectrum of $[ZnL_2]$ is not solvent dependent (thf or MeCN) and (*iii*) the crystal structures show the molecules to be centrosymmetric and, geometrically, almost within experimental error of D_{2h} symmetry. The ZINDO-derived electronic excited states up to 40.0×10^3 cm^{-1}, their pertinent oscillator strength, symmetry label, main character and polarization, are reported in Table 5. The first allowed state is calculated at 16.1×10^3 cm^{-1}; it is *y* polarized and comprised a mixture of the two configurations $(b_{2g})(a_u)$ and $(b_{1u})(b_{3g})$, derived from the four frontier orbitals; the other allowed state derived from a complementary mixture of the same configurations is $2B_{2u}$. Both $2B_{1g}$ and $4B_{1g}$ are the forbidden states, derived from the same four frontier orbitals, and have a mixture of the two forbidden configurations $(b_{2g})(b_{3g})$ and $(a_u)(b_{1u})$. These could eventually give an *x*- or *y*-intensity contribution *via* a vibronic mechanism, when an *x*- or *y*-allowed molecular vibration is excited (b_{3u} or b_{2u}, respectively). Other electronically forbidden transitions ($1B_{1g}$, $3B_{1g}$, B_{2g} and B_{3g}), L ⟶ M and d ⟶ d in character, are calculated in this region, but they will be undoubtedly absent in $[ZnL_2]$, given that this complex has a d^{10} metal configuration and is not expected to exhibit L ⟶ M charge-transfer transitions at low energy.

Note that intense *x*-polarized transitions are predicted in the B region. The *z*-polarized B_{1u} states, which have contributions from imino-nitrogen lone-pair p_y orbitals, responsible for σ-co-ordination, are calculated at even higher energy.

Assignment.—From a comparison of the spectral data (Table

4) and calculated transitions (Table 5), it is clear that the theoretical model by itself is not sufficiently adequate to interpret both energies and intensities. Two experimental factors could have contributed to the discrepancies: (*i*) intensity information from Kramers–Krönig transformations is not as quantitative as the energy information and (*ii*) as noted earlier, some depolarization may have occurred due to the triclinic habit of the crystal. Some features, however, such as the inversion of intensity ratio of Q and B bands may arise from an extensive mixing between states of the same or different symmetry, by means of suitable molecular vibrations. In this particular case, the *y*-allowed $1B_{2u}$ state could be coupled to $4B_{2u}$ by a total symmetric vibration (a_g) transferring some intensity from the B band to the *y*-polarized components of the Q band, or coupled to the *x*-allowed $1B_{3u}$ states by a b_{1g} vibration, transferring some intensity from the B band to the *x*-polarized component of the Q band. Such a mechanism, which accounts for the intensity stealing and mixed polarization, is well established,[16a] even for allowed, intense $\pi \longrightarrow \pi^*$ transitions in aromatic molecules.[16b,c] Invoking such a vibronic intraconfigurational interaction and taking into account the number of the calculated states for $[NiL_2]$, which are also appropriate for $[ZnL_2]$, all the components of the Q, B and N bands can be assigned, in a first approximation. Consequently, the three main vicinal components of the Q band have been interpreted as a superposition of vibrational overtones and/or combinations of numerous vibrations of mainly a_g (in *R*2 polarization) and b_{1g} (in *R*1 polarization) character of a single electronic transition ($^1A_g \longrightarrow {}^1B_{2u}$), rather than arising from the overlapping of different electronic transitions; however, the final state cannot be identified simply with the calculated $1B_{2u}$, but is instead a mixed state with other B_{2u} states *via* a_g vibration or B_{3u} states, perturbed by b_{1g} vibration ($B_{3u} \times b_{1g} = B_{2u}$). The low-intensity component at 19.45×10^3 cm^{-1}, instead, allowed only in *R*1 polarization, could well be a separate electronic transition, probably to the forbidden $2B_{1g}$ state, calculated at 15.2×10^3 cm^{-1} and partially made allowed by a b_{3u} molecular vibration. The B band originates from six electronic transitions;

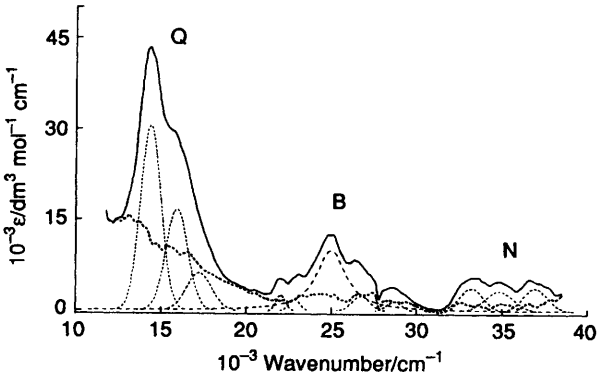

Fig. 6 Kramers–Krönig transformed spectrum of ZnL_2·4thf with the electric vector parallel to *R*2 and Gaussian analyses; (———) transformed experimental spectrum; (- - - -) Gaussian curve; (– – –) Lorentzian; (• • • •) residual

Table 4 Band-fitting parameters for the absorption spectra of Figs. 5 and 6 and possible assignment *

*R*2 spectrum			Assignment			*R*1 spectrum		
				Band label				
$\tilde{\nu}_{max}$	ε_{max}	Area				Area	ε_{max}	$\tilde{\nu}_{max}$
14.40	30.66	1.262				0.64	15.43	14.35
15.95	16.71	0.665	B_{2u}	Q	$B_{2u} \times B_{3u} \times b_{1g}$	0.64	12.04	15.95
17.25	6.20	0.258				0.24	4.85	17.40
					$1B_{1g} \times b_{3u}$	0.30	4.32	19.45
22.05								
22.85	2.58	0.030			$2B_{1g} \times b_{3u}$	0.11	3.86	23.35
25.00	1.89	0.024	B_{2u}		B_{3u}			
26.75	9.99	0.508	$B_{3u} \times B_{2u} \times b_{1g}$	B	B_{3u}	0.37	9.91	25.10
28.70	2.45	0.046	B_{2u}			0.290	6.85	27.35
	1.51	0.023	B_{2u}			0.060	2.33	29.95
33.20								
34.85	3.79	0.077	$B_{1u} \times B_{2u} \times b_{3g}$		$B_{1u} \times B_{3u} \times b_{2g}$	0.100	3.39	33.20
36.95	3.27	0.077	$B_{1u} \times B_{2u} \times b_{3g}$	N	$B_{1u} \times B_{3u} \times b_{2g}$	0.040	2.73	35.05
	3.79	0.072	$B_{1u} \times B_{2u} \times b_{3g}$		$B_{1u} \times B_{3u} \times b_{2g}$	0.040	2.33	36.50

* *R*1 and *R*2 spectra are those reported in Figs. 5 and 6, respectively; $\tilde{\nu}$ and ε are expressed in 10^3 cm^{-1} and 10^3 dm^3 mol^{-1} cm^{-1}, respectively.

Table 5 Calculated excited states for $[NiL_2]$ [a]

State	10^{-3} Energy/cm^{-1}	Oscillator strength	Polarization	Character
$1B_{1g}$ [b]	13.8	0	—	d ⟶ d
B_{3g} [b]	14.4	0	—	L ⟶ M
$2B_{1g}$	15.2	0	—	$\pi \longrightarrow \pi^*$
B_{2g} [b]	16.0	0	—	L ⟶ M
$1B_{2u}$	16.1	0.556	*y*	$\pi \longrightarrow \pi^*$
$3B_{1g}$ [b]	18.6	0	—	d ⟶ d
$4B_{1g}$	27.1	0	—	$\pi \longrightarrow \pi^*$
$2B_{2u}$	27.2	0.003	*y*	$\pi \longrightarrow \pi^*$
$3B_{2u}$	31.3	0.017	*y*	$\pi \longrightarrow \pi^*$
$1B_{3u}$	32.1	0.916	*x*	$\pi \longrightarrow \pi^*$
$4B_{2u}$	33.0	1.011	*y*	$\pi \longrightarrow \pi^*$
$2B_{3u}$	33.7	1.387	*x*	$\pi \longrightarrow \pi^*$
$3B_{3u}$	36.1	0.006	*x*	$\pi \longrightarrow \pi^*$
$1B_{1u}$	37.2	0.003	*z*	$\pi \longrightarrow \sigma^*$
$2B_{1u}$	38.0	0.019	*z*	$\pi \longrightarrow \sigma^*$

[a] From ref. 3. [b] State not appropriate for $[ZnL_2]$ (see text).

its prominent component at *ca.* 25.0 × 10^3 cm^{-1} is allowed to a different extent along *x* and *y*, probably because the corresponding final state is a mixture of the *x*-allowed $1B_{3u}$ state and the *y*-allowed B_{2u} state *via* a b_{1g} molecular vibration (again, $B_{2u} \times b_{1g} = B_{3u}$). Finally, the N band appears to consist of three transitions in each spectrum, which are consistent with the calculated transitions in this region; they are allowed in all the directions, mostly in the *z* direction, so that states of symmetry mostly B_{1u} contribute to them, having 'forbidden' components from mixing with B_{2u} and B_{3u} states, perturbed by b_{3g} ($B_{2u} \times b_{3g} = B_{1u}$) and b_{2g} vibrations ($B_{3u} \times b_{2g} = B_{1u}$), respectively.

Acknowledgements

We thank the Progetto Finalizzato Materiali of Consiglio Nazionale della Ricerce (CNR) for partial financial support. R. L. M. acknowledges the Donors of the Petroleum Research Fund administered by the American Chemical Society, Grant No. 25966-B3, and the National Science Foundation Inorganic, Bioinorganic, and Organometallic Chemistry Program, Grant No. CHE-9213251. The authors also thank Karen Jennings, Jun Kim and Dr. David Kramer of Franklin and Marshall College for their help in spectral calculations and C. Veroli of CNR for his assistance in the X-ray work.

References

1 M. Bonamico, V. Fares, A. Flamini and N. Poli, *Angew. Chem., Int. Ed. Engl.*, 1989, **28**, 1049.
2 M. Bonamico, V. Fares, A. Flamini and N. Poli, *Inorg. Chem.*, 1991, **30**, 3081.
3 S. Nakamura, A. Flamini, V. Fares and M. Adachi, *J. Chem. Phys.*, 1992, **96**, 8351.
4 *Chemistry of Functional Dyes*, eds. Z. Yoshida and T. Kitao, Mita Press, Tokyo, 1989, pp. 533–545; A. J. Bur, R. E. Lowry, S. C. Roth, C. L. Thomas and F. W. Wang, *US. Pat.*, 5 151 748, 1990.
5 A. Flamini and N. Poli, *US. Pat.*, 5 151 527, 1992.
6 A. R. Pray, *Inorg. Synth.*, 1954, **5**, 153.
7 SHELXTL PC Siemens Crystallographic Research System, Siemens Analytical X-Ray Instruments Inc., Madison, WI, 1990.
8 *International Tables for X-Ray Crystallography*, Kynoch Press, Birmingham, 1974, vol. 4.
9 M. Camalli, D. Capitani, G. Cascarano, S. Cerrini, C. Giacovazzo and R. Spagna, *Ital. Pat.*, 35403c/86, 1986.
10 B. G. Anex, *Mol. Cryst.*, 1966, **1**, 1.
11 A. J. Finney, M. A. Hitchman, C. L. Raston, G. Rowbottom and A. H. White, *Aust. J. Chem.*, 1981, **34**, 2061.
12 K. R. Adam, B. J. McCool, A. J. Leong, L. F. Lindoy, M. McPartlin, D. K. Uppal and P. A. Tasker, *J. Chem. Soc., Dalton Trans.*, 1990, 3435.
13 T. Ito, M. Kato and H. Ito, *Bull. Chem. Soc. Jpn.*, 1984, **57**, 2634.
14 E. Labisbal, J. A. Garcia-Vazques, C. Gomez, A. Macias, J. Romero, A. Sousa, U. Englert and D. E. Fenton, *Inorg. Chim. Acta*, 1993, **203**, 67; J. A. Castro, J. Romero, J. A. Garcia-Vazquez, A. Macias, A. Sousa and U. Englert, *Polyhedron*, 1993, **12**, 1391; J. Castro, J. Romero, J. A. Garcia-Vazques, M. L. Duran, A. Castineras, A. Sousa and D. E. Fenton, *J. Chem. Soc., Dalton Trans.*, 1990, 3255; N. W. Alcock, K. P. Balakrishnan, A. Berry, P. Moore and C. G. Reader, *J. Chem. Soc., Dalton Trans.*, 1988, 1089; W. Clegg, I. R. Little and B. P. Straughan, *J. Chem. Soc., Dalton Trans.*, 1986, 1283; L. Casella, M. E. Silver and J. A. Ibers, *Inorg. Chem.*, 1984, **23**, 1409; G. A. Nicholson, J. C. Petersen and B. J. McCormick, *Inorg. Chem.*, 1982, **21**, 3274; I. Sotofte and K. Nielsen, *Acta Chem. Scand., Ser. A*, 1981, **35**, 739; W. R. Sheidt and W. Dow, *J. Am. Chem. Soc.*, 1977, **99**, 1101.
15 P. Luger and J. Buschmann, *Angew. Chem., Int. Ed. Engl.*, 1983, **22**, 410; X. L. Luo, G. K. Schulte and R. H. Crabtree, *Inorg. Chem.*, 1990, **29**, 682.
16 (*a*) A. C. Albrecht, *J. Chem. Phys.*, 1960, **33**, 156; (*b*) A. C. Albrecht and W. T. Simpson, *J. Chem. Phys.*, 1955, **23**, 1480; (*c*) A. C. Albrecht, *J. Am. Chem. Soc.*, 1960, **82**, 3813.

Received 25*th July* 1994; *Paper* 4/04539D